Iranian Journal of Oil & Gas Science and Technology, Vol. 7 (2018), No. 3, pp. 32-52
http://ijogst.put.ac.ir

Advanced Analysis of Dew Point Control Unit of Hybrid Refrigeration Systems in Gas Refineries

Mahmoud Afshar* and Hamid Rad

[1] Assistant Professor, Department of Mechanical Engineering, Petroleum University of Technology, Mahmoudabad, Mazandaran, Iran
[2] M.S. Student, Department of Energy Systems Engineering, Petroleum University of Technology, Mahmoudabad, Mazandaran, Iran

Received: December 26, 2016; *revised*: February 16, 2017; *accepted*: March 17, 2017

Abstract

In this paper, an advanced analysis of a novel hybrid compression-absorption refrigeration system (HCARS) for natural gas dew point control unit in a gas refinery is presented. This unit separates the heavy hydrocarbon molecules in the natural gas, which is traditionally carried out by natural gas cooling in a compression refrigeration cycle (CRS). The power input required for the refrigeration cycle compressors is usually provided by gas turbines. The low efficiency of gas turbines and the excessive power required for running the CRS compressors have made it crucial to investigate different means to decrease the energy consumption of this cooling system.

The waste heat of gas turbines flue gas can be recovered and utilized as the heating source for running an absorption refrigeration system (ARS) to provide part of the needed cooling load; hence, a hybrid compression absorption refrigeration system (HCARS) is launched. In this work, the application of HCARS is extended to the Fajr-e-Jam gas refinery currently operating with a CRS, and an advanced exergetic analysis of the proposed ARS is performed to further improve the proposed system. The effect of different variables on the performance of the proposed HCARS is also inspected. The proposed system and these analyses are novel for the gas refinery dew point control unit. Real CRS operational data are utilized in all the investigations, and proper means are presented for the validation of the simulation results.

The proposed system resulted in 63% additional cooling capacity of the HCARS (12550 KW) in comparison to the current CRS (7670 kW) for the equal natural gas consumption, which overall saves about 50000 SCMD of natural gas. Based on the exergy analysis of all the equipment, the exergy efficiency of the proposed ARS is 0.155. In addition, the parametric study of the effects of the gas turbine flue gas exit temperature and flow rate, ambient temperature, partial load operation of CRS, absorption solution flow rate, and concentration on the HCARS performance is carried out. These studies should provide the information needed for operating the proposed system in different situations.

Keywords: Hybrid Refrigeration, Gas Refinery, Exergy Analysis, Performance

* Corresponding Author:
Email: mafshar@put.ac.ir

1. Introduction

To achieve a sustainable development, economic progress should be accomplished along with environment protection and social justice. The main engine for economic development is energy which should be provided as needed by different sectors of economy. Uncontrolled consumption of fuels to generate energy nowadays is not tolerated anymore, and many researchers around the globe are working to limit the fuel consumption for the protection of the environment. In this context, it is crucial that the energy intensive industries such as oil and gas operate efficiently. Gas refineries consume a vast amount of energy for sweetening, de-watering, pressurizing, and controlling the dew point of the natural gas delivered to the gas trunk lines.

In order to minimize gas condensation in natural gas trunk pipelines, the heavy molecules of the natural gas are separated in the dew point control unit in gas refineries. Traditionally, this task has been carried out by natural gas cooling in a compression refrigeration cycle (CRS). The power required to operate the huge compressors of CRS is usually provided by gas turbines; with relatively low efficiency and considerable flue gases energy losses through its stacks.

The main idea is to recover the flue gas waste heat and utilize it as the heat energy source for running an absorption refrigeration system (ARS) to provide part of the cooling load needed for natural gas dew point reduction. Therefore, in this work a hybrid compression absorption refrigeration system (HCARS) is proposed for industrial refrigeration system, specifically for gas refineries dew point control units.

The idea has been worked out in labs or for other industrial and commercial applications, but to the best of our knowledge, it has not been implemented for gas refineries. Benjamin Brant et al. (1998) have investigated this system for a particular application in oil refineries. The refrigeration unit was designed to provide refrigeration for two process units at the refinery while utilizing waste heat as the energy source. The ARS enabled cooling of the gas up to -31.7 °C, thereby recovering 45% of high molecular weight hydrocarbons (Kalinowski et al., 2009).

Priedeman and Christensen (1999) presented a general ammonia-water absorption heat pump cycle that was modeled and tested. The simulation results were found to be in close agreement with the experimental data (Jianbo et al., 2013).

A.K. Pratihar et al. (2011) simulated an ammonia-water HCARS by incorporating detailed heat and mass transfer calculations in the absorber and desorber of the system. They studied the effect of solution heat exchanger area on the COP. With an increase in the solution heat exchanger area (almost tripled), COP increased initially, reached a maximum value at 39%, and then decreased (Pratihar et al., 2012).

N.A. Darwish et al. (2013) analyzed the absorption–refrigeration water–ammonia system using Aspen Plus flow sheet simulator. Very good agreement between the simulation results and the experimental measurements was found out.

Considering the promising results of the above studies, the idea of a HCARS in a gas refinery dew point control unit is investigated in this research. In this particular application, there are two refrigerants for CRS and ARS cycles, namely propane and ammonia, which is not the case in previous investigations. Furthermore, an exergy analysis is performed in this research, which is a step forward in this field to find out further possible improvements in overall HCARS efficiency. Additionally, to make a meaningful comparison between the performance of the available CRS and the proposed HCARS, COP values are calculated based on a new understanding in this paper. For the proposed system, to be beneficial to the gas refinery, real operational data of the available CRS had to be observed, and corresponding limitations had to be specified and watched.

A brief discussion of the thermodynamic analysis of the current and the proposed extension to the existing dew point control unit of Fajr-e-Jam gas refinery propane CRS is presented first. In the second part of the paper, the exergy analyses of the proposed ARS are discussed. For a better understanding of system performance in different operational conditions, the parametric studies of the important parameters affecting the overall performance of the proposed HCARS system are explained in the last part of the paper.

2. Proposed HCARS

The current dew point control unit in Fajr-e-Jam gas refinery is utilizing propane CRS, in which the compression is performed by six parallel interconnected turbo-compressors run by AVON ROLLS ROYCE 11500 HP gas turbines.

The ARS is placed parallel to the available propane refrigeration cycle in the proposed HCARS, Figure 1. Exhaust flue gas of the gas turbine is recovered in a heat recovery steam generator (HRSG) to be used for the production of the high pressure steam which supplies required ARS heat demand. All calculations are based on CRS real operational conditions and carried out by HYSYS (v7.2) for the proposed ARS. Full details are available elsewhere (Rad, 2016).

In the analysis, the principles of mass conservation, energy conservation, and the second law of thermodynamics are applied to each component of the system. Every component was considered as a control volume, taking into account the heat transfer, work interaction, and inlet and outlet streams.

The governing equations for mass conservation are defined by:

Mass balance:

$$\sum \dot{m}_i - \sum \dot{m}_o = 0 \tag{1}$$

Mass balance for ammonia:

$$\sum \dot{m}_i x_i - \sum \dot{m}_o x_o = 0 \tag{2}$$

where, x_i and x_o correspond to the inlet and outlet ammonia mass fractions.

Energy balance:

The first law of thermodynamics yields the energy balance of each component of the whole system in following form:

$$\dot{Q} - \dot{W} = \sum \dot{m}_o h_o - \sum \dot{m}_i h_i \tag{3}$$

Entropy balance:

$$\dot{S}_{gen,K} = \sum \dot{m}_e s_e - \sum \dot{m}_i s_i - \frac{\dot{Q}_K}{T_K} \tag{4}$$

The equations are subjected to the following assumptions:

- Steady state;
- Pure ammonia in the evaporator;
- Negligible pressure drops and heat losses to the environment;
- Saturated vapor at the purification column's exit;

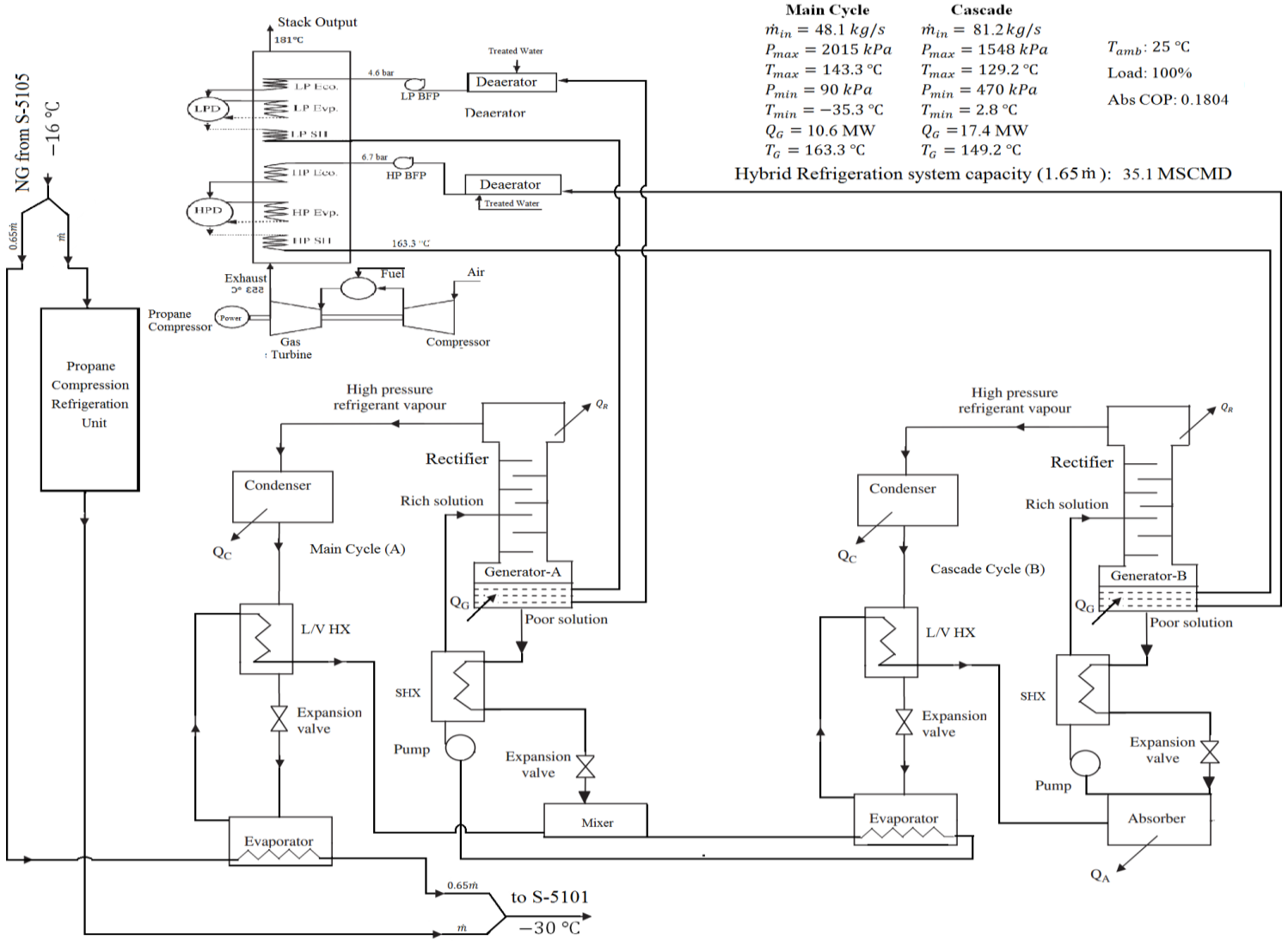

Figure 1
Proposed hybrid refrigeration system layout.

The main operational parameters needed for the analysis of the proposed ARS extension are the gas turbine flue gas mass flow rate and temperature at the gas turbine stack entrance; the nominal temperature is 533 ℃. The recorded temperatures in the log sheets in 4 different months were collected (about 11000 recorded data). The convenient value to represent the flue gas exhaust temperature was determined to be 540 °C (Rad, 2016). The flue gas mass flow rate is equal to the fuel consumption rate in a turbo-compressor plus its air intake (assuming no leakages). The gas turbine flue gas operational data are shown in Table 1.

Table 1
Exhaust flue gas operational specifications.

Parameter	Value
Exhaust flue gas temperature	540 ℃
Exhaust flue gas mass flow rate	75.5 kg/s
Exhaust flue gas pressure	101.3 kPa

As shown in Figure 1, the gas turbine exhaust flue gas heat is transferred to a water stream in a HRSG to produce steam which is later used as the heat source in the generator of absorption refrigeration cycle. In a cascade absorption refrigeration cycle, as schematically shown in Figure 1, there are a main cycle and a cascade cycle, utilizing high pressure and low pressure steams respectively. Therefore, in the HRSG, high and low pressure steam streams are produced as shown in Figure 1 (H.P. and L.P.). The HRSG is designed so that any changes in flue gas conditions do not affect the steam streams pressure or temperature; only the mass flow rate of the steam streams change.

The specifications of the steam produced in the HRSG are shown in Table 2, and the assumptions for the simulation of hybrid refrigeration system are listed in Table 3.

The simulation results (as obtained by Aspen-Hysys) are shown in Table 4. The 4.49 MW cooling rate of the ARS main cycle evaporator is utilized for cooling natural gas in parallel to the available CRS 7.26 MW cooling rate; hence, the HCARS cooling rate will be 7.26 + 4.49 = 11.75 MW, which is 1.62 times larger than the original CRS cooling capacity at the same amount of fuel gas consumption.

Table 2
The steam produced in the HRSG specifications.

Parameter	Value	Parameter	Value
HP steam temperature	163.4 ℃	LP steam temperature	149.3 ℃
HP steam pressure	670 kPa	LP steam pressure	465 kPa
HP steam mass flowrate	4.9 kg/s	LP steam mass flowrate	8.32 kg/s
HRSG effectiveness	0.9	Minimum allowable stack temperature	179 ℃

Table 3
Assumption for the simulation of hybrid refrigeration system.

Parameter	Value
Environment temperature (℃)	25
Evaporator temperature (℃)	-35
Flue gas temperature (℃)	540
Isentropic efficiency of pumps	0.8
Isentropic efficiency of turbines	0.3
Minimum temperature of flue gas (℃)	179
Minimum pressure (kPa)	90
Maximum pressure (kPa)	2015

The ARS COP is defined as the useful heat rate from evaporator ($\dot{Q}_E$) divided by the required heat rate to the generator $\dot{Q}_G$ [26].

$$COP_{Abs} = \frac{\dot{Q}_E}{\dot{Q}_G} = \frac{[\dot{m}(h_e - h_i)]_{ammonia}}{[\dot{m}(h_i - h_e)]_{steam}} \tag{5}$$

The COP of the compression refrigeration system is defined as:

$$COP_{Comp} = \frac{\dot{Q}_{Evap}}{\dot{W}_{Comp}} \tag{6}$$

To provide proper ground for the comparison of the original CRS and the proposed HCARS performance, in this research, the COP definition is modified as follows:

$$COP_{CRS} = \frac{(\dot{Q}_{Evap})_{Com}}{Heating\ Energy\ of\ fuel\ gas} \tag{7}$$

The COP of ARS is defined as:

$$COP_{ARS} = \frac{(\dot{Q}_{Evap})_{Abs}}{Input\ Heating\ Energy\ of\ flue\ gas} \tag{8}$$

Also, assuming that the only source of heat needed for ARS is the GT flue gas, and ARS pump power is negligible, the COP of HCARS is given by:

$$COP_{Hybrid} = \frac{\left(\dot{Q}_{Evap}\right)_{Abs} + (\dot{Q}_{Evap})_{Com}}{Heating\ Energy\ of\ fuel\ gas} \tag{9}$$

The COP's of CRS (from Equations 5, 6, and 9), the (standalone) ARS, and the proposed HCARS, based on CRS nominal and operational conditions, are tabulated in Table 5.

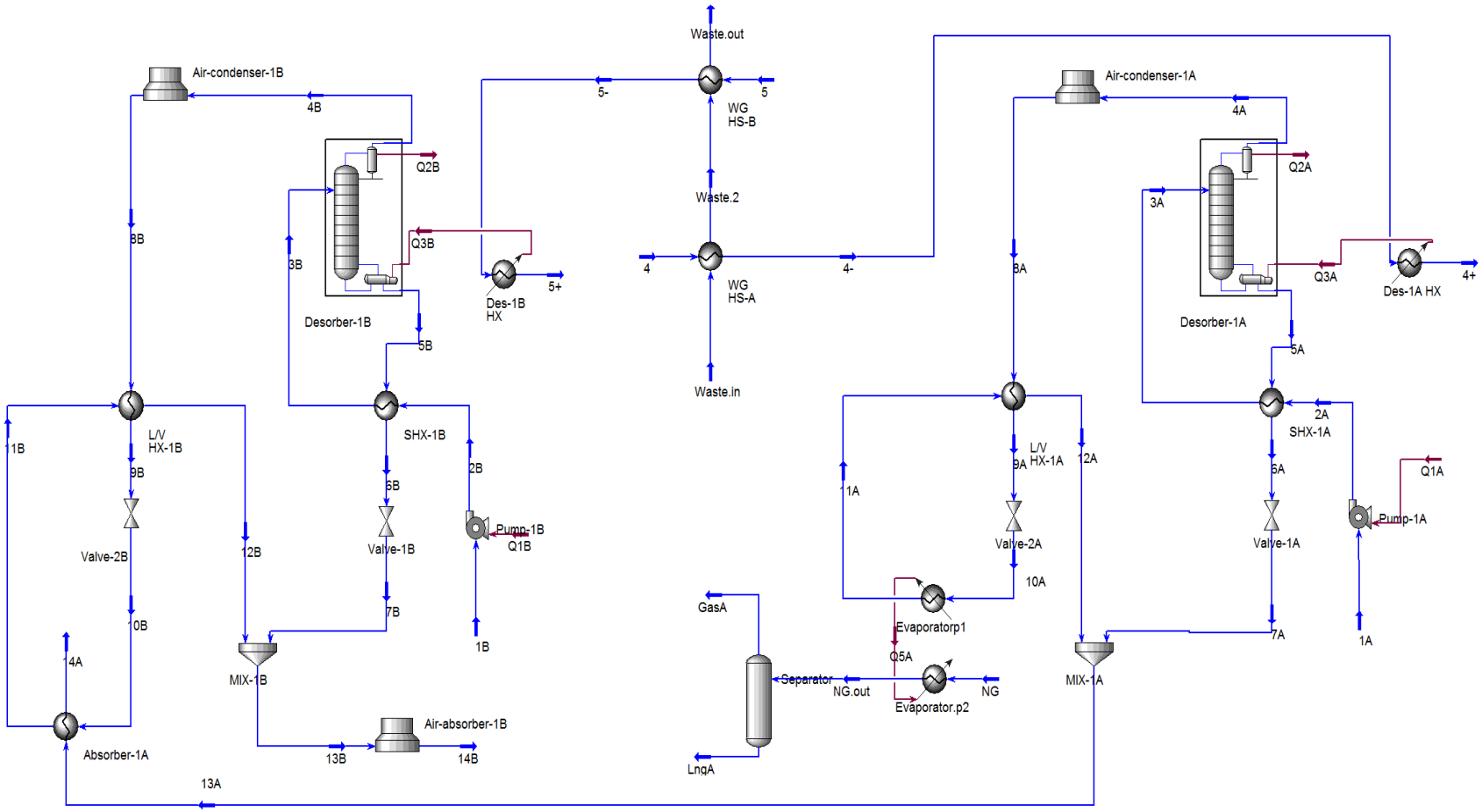

Figure 2
Process diagram of the suggested cascade absorption cycle for Fajr-e-Jam dew point unit.

Table 4
Streams data of suggested cascade absorption cycle for Fajr-e-Jam dew point unit.

Stream	**1A**	**2A**	**3A**	**4A**	**5A**	**6A**	**7A**	**8A**	**9A**	**10A**	**11A**	**12A**	**13A**	**14A**
T (℃)	12.64	12.86	126	63.9	143.4	18.48	18.91	50.05	-25	-35	-34.79	31.82	23	12.61
P **(kPa)**	91.4	2020	2020	2020	2020	2020	91.4	2015	2015	91.4	91.4	91.4	91.4	91.4
$\dot{m}$ **(kg/s)**	42.3	42.3	42.3	3.9	38.4	38.4	38.4	3.9	3.9	3.9	3.9	3.9	42.3	42.3
X_{NH3}	0.33	0.33	0.33	0.998	0.259	0.259	0.259	0.998	0.998	0.998	0.998	0.998	0.33	0.33
Quality	0	0	0	1	0	0	0	0	0	0.0342	0.84	1	0.0865	0
From	Abs-A	Pump-A	SHX-A	Des-A	Des-A	SHX-A	Vlv-1A	Con-A	L/V-A	Vlv-2A	Eva	L/V-A	MIX-A	Abs-A
To	Pump-A	SHX-A	Des-A	Con-A	SHX-A	Vlv-1A	MIX-A	L/V-A	Vlv-2A	Eva	L/V-A	MIX-A	Abs-A	Pump-A
Stream	**1B**	**2B**	**3B**	**4B**	**5B**	**6B**	**7B**	**8B**	**9B**	**10B**	**11B**	**12B**	**13B**	**14B**
T **(℃)**	57.97	56.15	112.3	56.48	129.3	67.36	69.83	40.21	8.55	0.0	0.6	21.93	69.84	57.97
P **(kPa)**	424	1550	1550	1550	1550	1550	424	1550	1550	424	424	424	424	424
$\dot{m}$ **(kg/s)**	71.4	71.4	71.4	6.6	64.8	64.8	64.8	6.6	6.6	6.6	6.6	6.6	71.4	71.4
X_{NH3}	0.33	0.33	0.33	0.998	0.259	0.259	0.259	0.998	0.998	0.998	0.998	0.998	0.33	0.33
Quality	0	0	0	1	0	0	0	0	0	0.031	0.9136	0.9975	0.0861	0
From	Abs-B	Pump-B	SHX-B	Des-B	Des-B	SHX-B	Vlv-1B	Con-B	L/V-B	Vlv-2B	Abs-A	L/V-B	MIX-B	Abs-B
To	Pump-B	SHX-B	Des-B	Con-B	SHX-B	Vlv-1B	MIX-1B	L/V-B	Vlv-2B	Abs-A	L/V-B	MIX-B	Abs-B	Pump-B

Stream	**4**	**4-**	**4+**	**Flue gas**	**5**	**5-**	**5+**	**Stack. Out**
T **(℃)**	163.3	163.3	163.3	540	149.2	149.2	149.2	181
P **(kPa)**	670.8	670.8	670.8	101.3	466	466	466	101.3
$\dot{m}$ **(kg/s)**	4.9	4.9	4.9	75.5	8.32	8.32	8.32	75.5
Composition	Water	Water	Water	Air	Water	Water	Water	Air
Quality	0	1	0	1	0	1	0	1

Table 5
COP values for different refrigeration schemes based on CRS nominal and operational conditions,

	COP based on CRS nominal conditions	**COP based on CRS operational conditions**
Compression refrigeration system	0.1934	0.1797
Absorption refrigeration system	0.1808	0.1804
Hybrid refrigeration system	0.3202	0.2938

The COP of HCARS is about 64% more than the available CRS (1167 kW extra cooling at the same fuel consumption rate). These results indicate the feasibility of the proposed HCARS for natural gas cooling in the dew point unit of the Fajr-e-Jam gas refinery under current CRS real working conditions. Hence, the first goal of this research is achieved. The full details are available elsewhere (Rad, 2016; Afshar and Rad, 2016).

3. Advanced analysis

In an effort to further improve the performance of the proposed HCARS two advanced analyses were carried out in this research. An exergy analysis of the main equipment of the ARS and a parametric study on the influential parameters affecting the ARS as well as the HCARS performances were performed. It should be noted that since the CRS is already operational, it is hardly beneficial to carry out these analyses for this system.

3.1. Exergy analysis

The purpose of the exergy analysis is to identify the sources of the thermodynamic inefficiencies and to find out the direction of improvement in the overall efficiency of the system through design changes. Once the process analysis is conducted and the proposed system process data are obtained, the exergy of the main equipment of the system and global exergy efficiency are evaluated. Overall exergy performance of the ARS is studied as a function of the exergetic behavior of each component, which specifies the origins of irreversibility.

Considering that the available CRS is already operating, and any possible modification in this system is hardly possible, in this section the analysis is carried out for ARS only, and the exergetic efficiencies of all the ARS components are calculated. Therefore, for improved efficiency, the engineers may focus on the more relevant components of the ARS.

a. Components of exergy

In the absence of nuclear, magnetic, electrical, and surface tension effects, the total exergy of the system (E) can be divided into four components: physical exergy (E_{PH}), kinetic exergy (E_K), potential exergy (E_{PT}), and chemical exergy (E_{CH}). If the kinetic and potential exergy are assumed to be negligible (Kotas, 1985), one may obtain:

$$E = E_{PH} + E_{CH} \tag{10}$$

$$E_{PH} = (h - h_0) - T_0.(s - s_0) \tag{11}$$

$$E_{CH} = \frac{x_n}{M_a}.e_a^{-ch} + \frac{1-x_n}{M_w}.e_w^{-ch} \tag{12}$$

where, x is the mole fraction of each component in the mixture, and M is the molecular weight of each component.

Exergy inputs (fuel exergy, $\dot{E}_F$) derived from the energy source transforms into exergy output (product exergy, $\dot{E}_P$) and destroyed exergy (exergy destruction, $\dot{E}_D$), and the remaining is the loss of exergy ($\dot{E}_L$).

Exergy destruction is the amount of exergy lost due to irreversibilities and cannot be used anywhere. The exergy loss is the amount of exergy that is wasted from the system under consideration, but it can be useful to other systems. The exergy destruction can be calculated by the exergy balance.

Exergy destruction at the individual component level is calculated using the following equation:

$$\dot{E}_{D,k} = \sum_{in} \dot{m}(h - T_0 s) - \sum_{out} \dot{m}(h - T_0 s) \tag{13}$$

where, T_0 is a reference temperature maintained at $293.15\,K$ throughout this study. It is noted that the definition of the exergy destruction rate accounts for both the physical and chemical exergy of the fluid streams, as suggested by Palacios Bereche et al., which is also consistent with the approach of Morosuk et al. (2014).

A detailed exergy analysis includes the calculations of exergy destruction, exergy loss, exergetic efficiency, exergy destruction ratios in each component of the system along with the overall system, and second law efficiency for the cycle. Mathematically, these are expressed as follows:

$$\dot{E}_D = \dot{E}_F - \dot{E}_P - \dot{E}_L \tag{14}$$

$$\varepsilon = \frac{\dot{E}_P}{\dot{E}_F} = 1 - \left[\frac{\dot{E}_D + \dot{E}_L}{\dot{E}_F}\right] \tag{15}$$

Exergy of ARS streams (calculated based on the process simulation results, listed in Table 4) are shown in Table 6.

Table 6
Exergy of ARS streams (Figure 2).

Stream	Exergy (kW)	Stream	Exergy (kW)	Stream	Exergy (kW)	Stream	Exergy (kW)
1A	315729.6	**9A**	88315.8	**1B**	533864.6	**9B**	148983.2
2A	315847.5	**10A**	88293.3	**2B**	533983.4	**10B**	148960.1
3A	318864.3	**11A**	87055.9	**3B**	537170.1	**11B**	148297.9
4A	88633.3	**12A**	86754.1	**4B**	149427.8	**12B**	148231.6
5A	230164.4	**13A**	316544.3	**5B**	387305.5	**13B**	535620.8
6A	226466.2	**14A**	315729.6	**6B**	383526.7	**14B**	533863.7
7A	226359.1	**8A**	88243.8	**7B**	383437.6	**8B**	148959.5

b. Exergetic efficiency of ARS

The rate of fuel exergy ($\dot{E}_{Fuel}$), the rate of product exergy ($\dot{E}_P$), the rate of destruction exergy ($\dot{E}_D$), and the rate of loss exergy ($\dot{E}_L$) for all the components of ARS are calculated using the data shown in Table 3. Four other parameters, i.e. exergy destruction ratio (Y_D), exergy destruction ratio (Y_D^*), exergy loss ratio (Y_L), and exegetic efficiency are also calculated based on the data shown in Table 5. The values of these parameters for the proposed ARS components are tabulated in Table 7.

Table 0
Exergetic destruction, loss, and efficiency using EDM.

Component	$\dot{E}_{Fuel}$ kW	$\dot{E}_P$ kW	$\dot{E}_D$ kW	$\dot{E}_L$ kW	Y_D %	Y_L %	Y_D^* %	ε %
Pump (A)	140.3	117.9	22.4	0	0.29	0	0.56	**84.03**
Generator (A)	2944.0	2749.7	194.3	0	2.59	0	4.85	**93.40**
Rectifier (A)	95040.1	94643.9	396.2	0	5.28	0	9.89	**99.58**
SHX (A)	3698.6	3016.8	681.8	0	9.08	0	17.02	**81.57**
Condensor, Evaporator-Assembly (A)	1626.9	943.7	301.9	381.3	4.02	5.08	7.54	**58.01**
L/V HX (A)	301.9	72.1	229.8	0	3.06	0	5.74	**23.86**
Absorber (A)	622.2	513.7	108.5	0	1.44	8.29	2.71	**82.56**
Pump (B)	140.1	117.9	22.2	0	0.29	0	0.55	**84.15**
Generator (B)	4406.8	4132.3	274.5	0	3.65	0	6.85	**93.77**
Rectifier (B)	156300.5	156072.9	227.6	0	3.03	0	5.68	**99.85**
SHX (B)	3778.8	3186.7	592.1	0	7.89	0	14.78	**84.33**
Condensor, Evaporator-Assembly (B)	1100.6	223.6	460.2	416.8	6.13	5.55	11.49	**20.32**
L/V HX (B)	66.3	23.7	42.6	0	0.57	0	1.06	**35.74**
Absorber (B)	535620.8	533863.7	209.6	1531.3	2.79	20.40	5.23	**99.67**
Overall system	**7505.2**	**1167.3**	**4005.3**	**2329.4**	**53.36**	**31.9**	**100**	**15.55**

The first exergy destruction ratio ($Y_{D,k}$) compares the exergy destruction in the k^{th} component with total exergy supplied to the system using the following equation:

$$Y_{D,k} = \dot{E}_{D,k} \Big/ \dot{E}_{F,tot} \tag{16}$$

The second exergy destruction ratio $Y_{D,k}^*$ compares the exergy destruction in the k^{th} component with total exergy destruction in the system.

$$Y_{D,k}^{*} = \dot{E}_{D,k} \Big/ \dot{E}_{D,tot} \tag{17}$$

The two exergy destruction ratios are useful for comparisons among various components of the same system. The first exergy destruction ratio can also be invoked for comparisons among similar components of different systems using the same, or closely similar, fuels.

The exergy loss ratio, $Y_{L,k}$, is defined as the ratio between the exergy loss in the k^{th} component and the total exergy supplied to the system.

$$Y_{L,k} = \dot{E}_{L,k} \Big/ \dot{E}_{F,tot} \tag{18}$$

The proposed ARS total input exergy and exergy destruction rates are 7505 kW and $4005\ kW$ respectively. Only 15.55% (1167 kW) of the input exergy is converted to cooling as the system useful output, while the remaining exergy is either lost to the environment (31.1% equal to 2394.4 kW) or destructed due to irreversibility in the various components of the system (53.36% equal to 4005.3 kW).

As shown in Figure 3, the exergetic efficiencies of the rectifiers and absorbers are the highest, and the exergetic efficiencies of condenser and evaporator assemblies and liquid/vapor heat exchangers are the least.

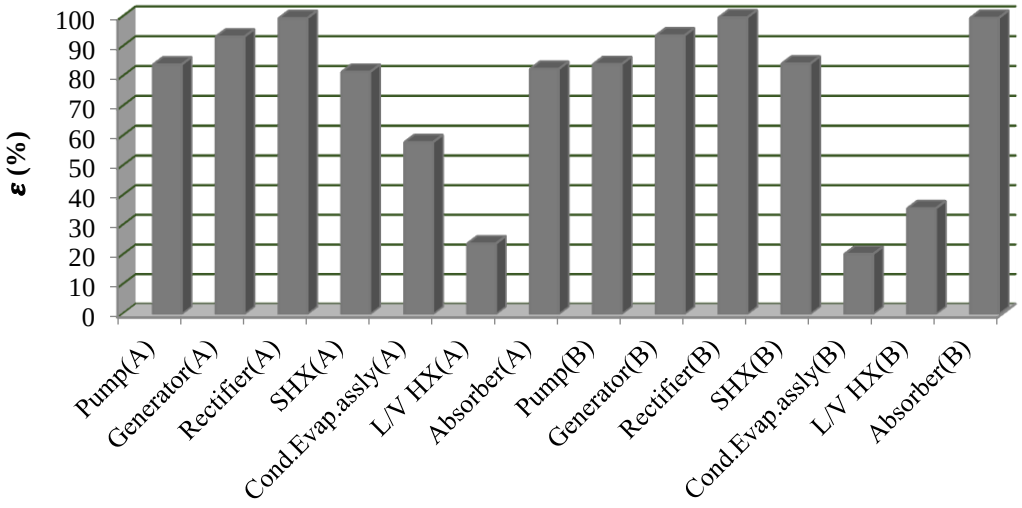

Figure 3
Exergetic efficiency of ARS components.

The highest total exergy destruction is found in SHX-A which is equal to 9.08% of the total exergy destruction of the system. The second highest exergy destruction is found out to be in the SHX-B, which amounts to 592.1 kW, equivalent to 7.89% of the total exergy destruction.

The exergetic efficiency for condenser-evaporator assembly and L/V HX of the main and cascade cycles

are almost low. The reason for the low exergetic efficiency of condenser-evaporator assembly may be attributed to the large temperature difference between the working fluid and brine in the evaporator and the working fluid and cooling air in the condenser. Similarly, the high temperature difference between both fluids and relatively very low mass flow rate of gaseous ammonia from the evaporator compared to the condensed ammonia from the condenser may be the reason for the poor exergetic efficiency of L/V HX.

4. Parametric study

To investigate the performance of the proposed HCARS system under different conditions, parametric studies of the influential parameters are carried out. These analyses would help the process engineers in charge of unit to make better decisions for the design of the proposed ARS system considering different real operational conditions.

4.1. Effect of solution mass flowrate on COP

The effect of ammonia-water solution mass flow rate changes on COP of the ARS is shown in Figure 4, assuming constant ammonia concentration. Also, it is assumed that the ratio of solution mass flow rates in two cycles A and B pumps is kept fixed (1.6887). As seen, the COP increases, almost, in direct proportion to the solution mass flow rate.

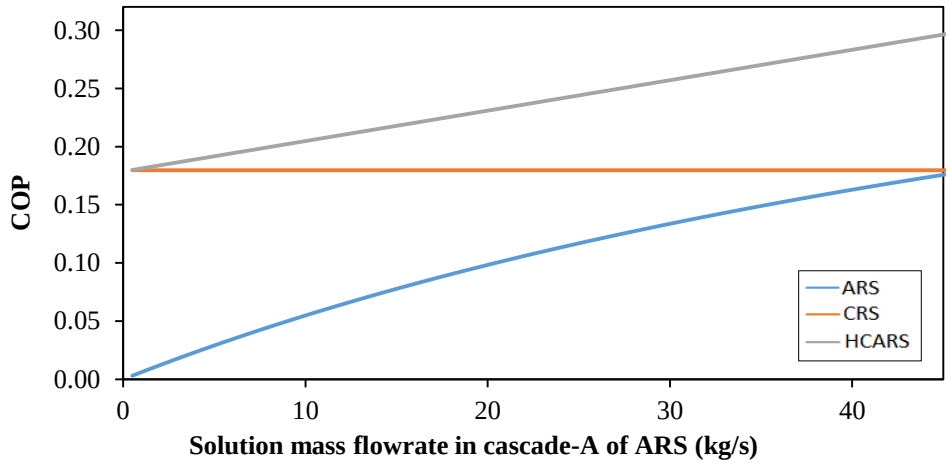

Figure 4
The effect of solution mass flow rate on COP.

4.2. Exhaust flue gas temperature and mass flowrate

The effects of gas turbine exhaust flue gas temperature and mass flow rate changes (heat source for absorption cycle) on the cooling rate of cascade ARS are shown in Figures 5 and 6 respectively. As can be seen, the evaporator cooling load is in direct proportion with the exhaust flue gas temperature; its mass flow rate and the ratios are almost linear too.

4.3. Ammonia concentration in rich solution

The effects of ammonia concentration in the rich solution on absorber-A working temperature and ARS

COP are shown in Figure 7. The same results are obtained for absorber-B as well.

To keep with the required cooling load, the reduction of the ammonia concentration should be compensated with an increase in pump mass flowrate, which in turn will reduce cycle COP; therefore, larger equipment should be used. The exit temperature of the absorber solution increases as the ammonia concentration falls, and there is a trade-off for ARS where the concentration should be set, which benefits both technically and economically. The recommended value of ammonia concentration in solution for these cases is 33 to 34 percent.

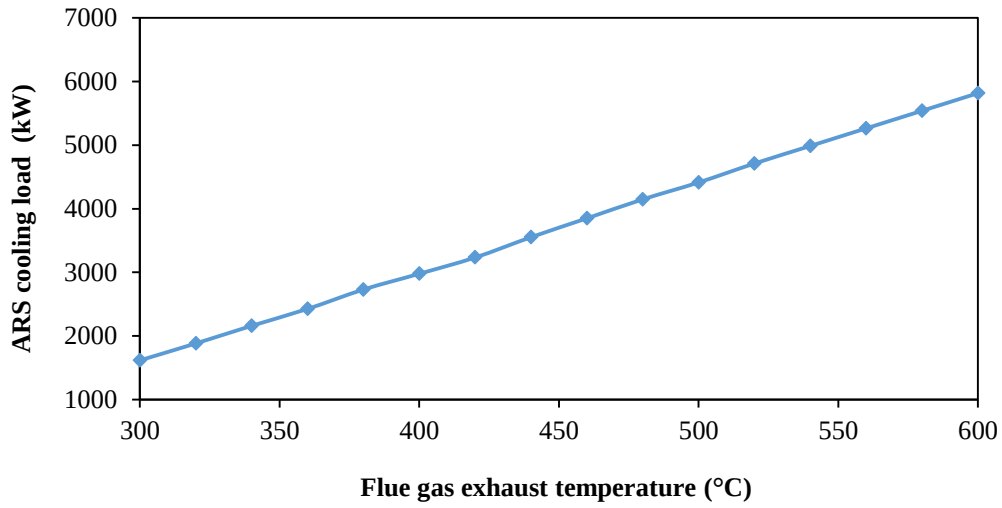

Figure 5
The effect of GT flue gas exhaust temperature on ARS cooling rate.

As expected, any decreases in these values drop heat energy recovery in HRSG; therefore, the cooling capacity of ARS decreases directly as well.

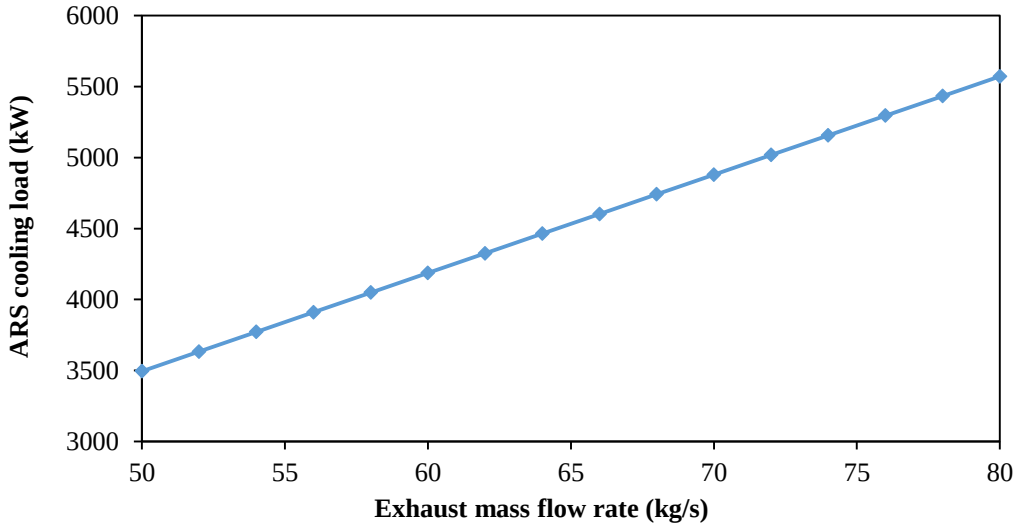

Figure 6
The effect of flue gas mass flow rate on ARS cooling rate.

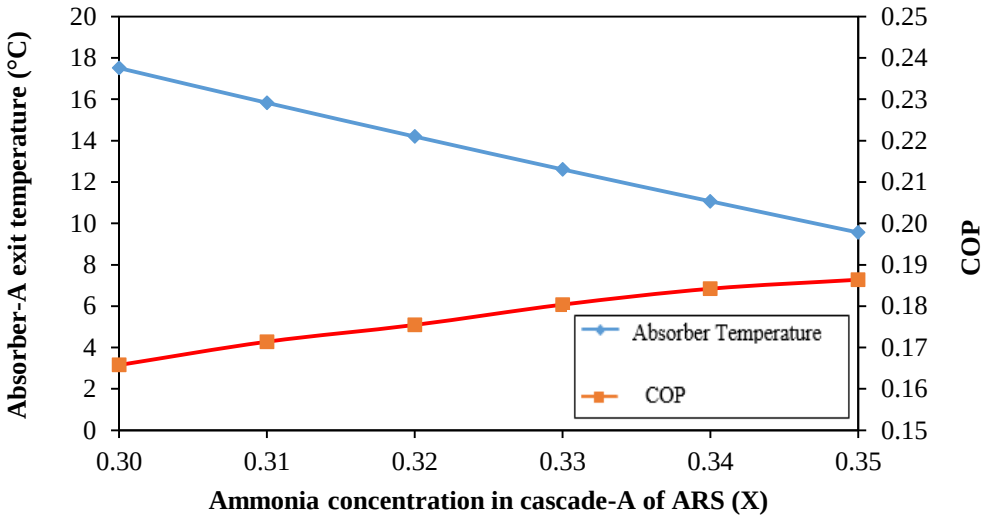

Figure 07
The effect of ammonia concentration on Absorber-A exit temperature and ARS COP.

4.4. Effect of ambient temperature

The effect of ambient temperature on the performance of the air condensers is shown in Figure 8. As the condenser heat load is constant, changes in ambient temperature, and hence, ΔT_{LMTD}, adversely change the UA values. If the ambient temperature increases more than the design limits, the fluid pressure in desorber could increase; thus, the condenser temperature rises to ambient temperature, which would reduce the COP of ARS. The effects of desorber A and B pressures on the COP of the ARS are shown in Figures 9 and 10 respectively.

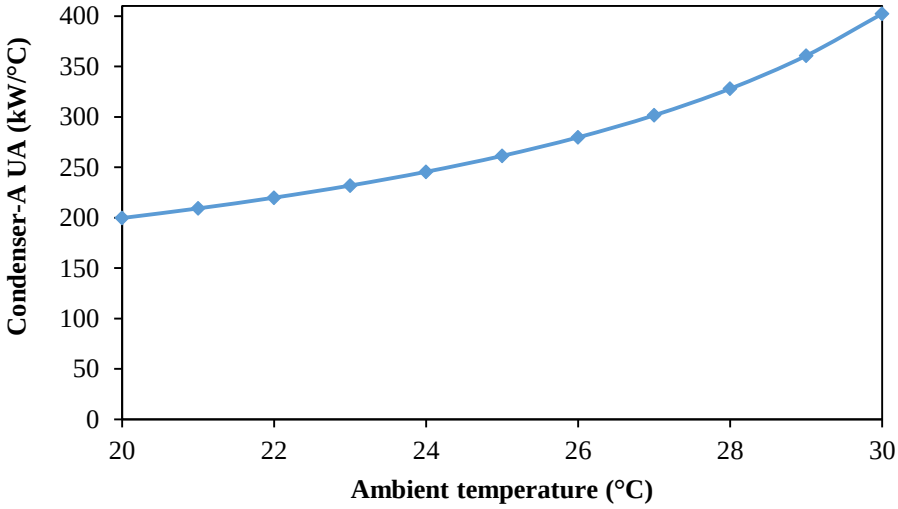

Figure 8
The effect of ambient temperature on the UA of condenser-A.

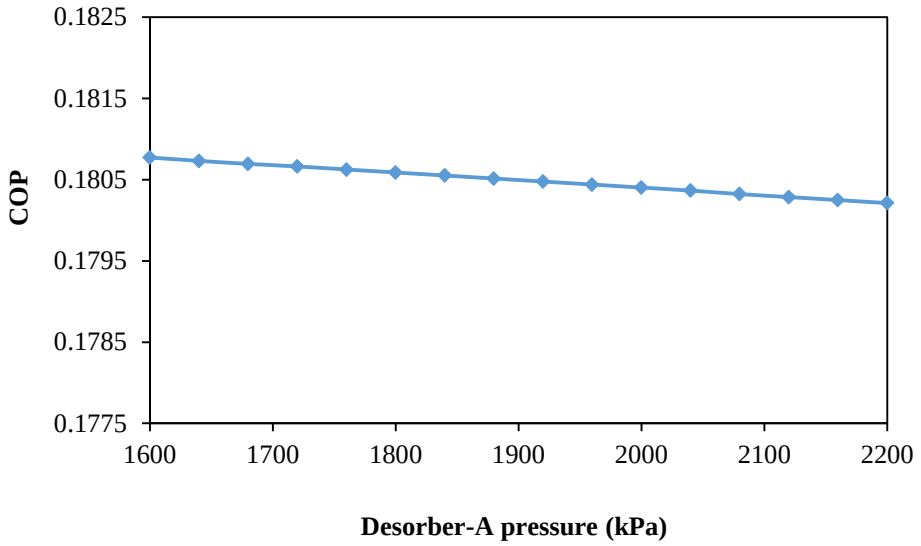

Figure 9
The effect of desorber-A working pressure on ARS COP.

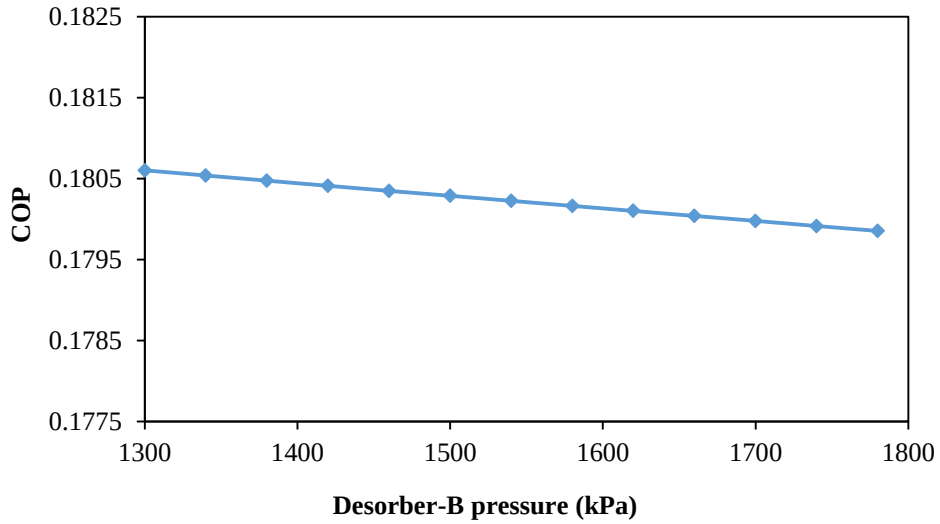

Figure 10
The effect of desorber-B working pressure on ARS COP.

4.5. Effect of partial load operation of CRS

The effect of partial load operation of the available CRS on the performance of ARS is shown in Figure 11. The real collected Far-e-Jam refinery operational data are up to the 75% of the nominal CRS working condition, and they have been extrapolated to 50% extent (the exhaust flue gas temperature and mass flow rate are obtained with second order regression). The propane mass flow rate is changed to alter the CRS cooling rate.

The field data show that the reduction of CRS cooling load results in a direct reduction of the flue gas

mass flow rate, while its temperature increases. Therefore, the increase in flue gas temperature to some degree compensates for the drop in its mass flow rate. Indeed, despite a reduction in CRS cooling rate, the ARS cooling rate remains almost unchanged and works near full load condition.

As shown in Figure 11, the ARS cooling load changes are within ±5% of the ARS full load operation. Also, the COP of ARS, CRS, and HCARS in partial cooling load of CRS are shown in Figure 12.

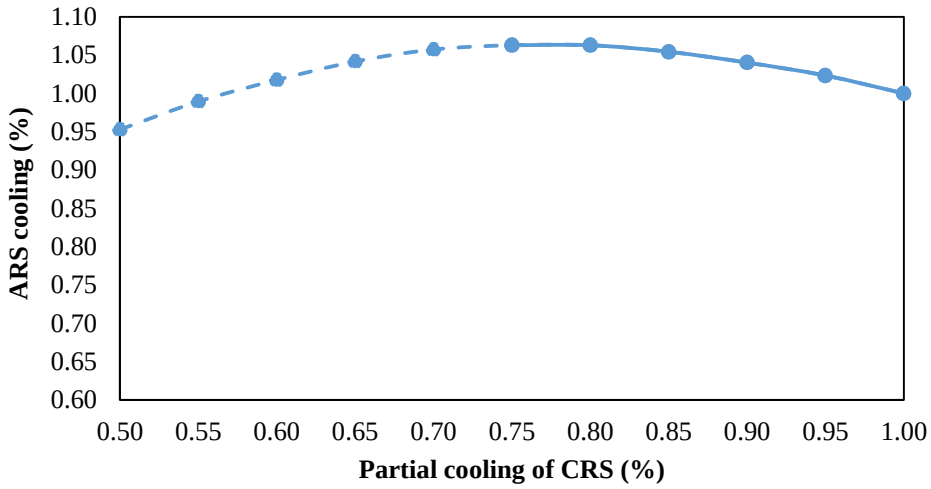

Figure 11
Cooling rate of ARS at partial cooling rates of CRS.

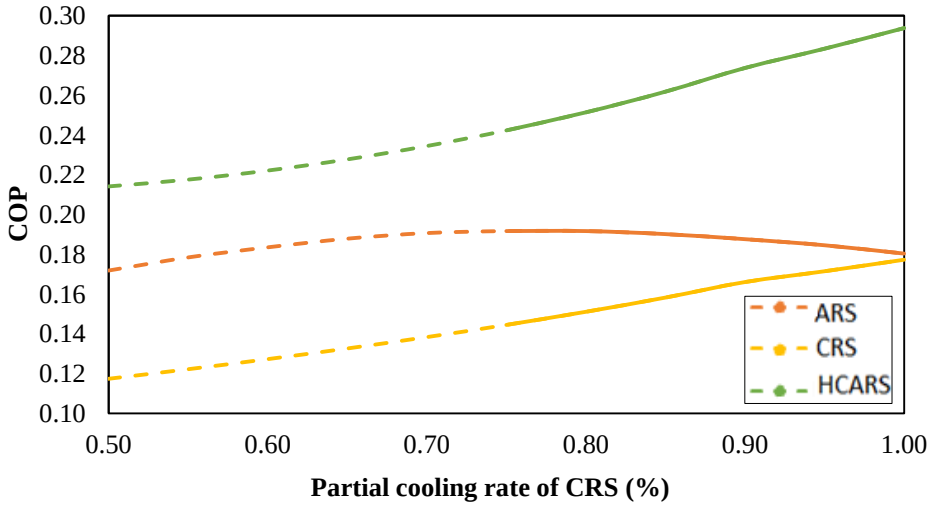

Figure 12
COP in partial load operation of CRS.

5. Conclusions

The energy efficiency of gas turbines in the dew point units of gas refineries can be enhanced considerably by using an ARS in conjunction with the available CRS to convert waste heat into useful cooling. A

feasibility analysis of a proposed HCARS for the dew point unit of gas refineries is carried out in this paper, and in addition, the advanced analyses for the improved HCARS are performed.

The worked out proposed HCARS resulted in 63% additional cooling capacity (12550 kW) in comparison to the current operating CRS (7670 kW) for the same fuel gas consumption, and overall about 50000 SCMD of natural gas could be saved by the possibility of shutting off one of the operational turbo-compressors; the COP of the proposed HCARS is 0.2938.

In advanced analysis, an exergy analysis is carried out to investigate the potential improvement in proposed hybrid system. From total exergy supplied to the ARS, 15.55% is converted to useful product, 53.36% is destroyed, and the 31.1% is lost to the environment.

In addition, the parametric study of the effect of the gas turbine flue gas exit temperature and flow rate on this system performance is carried out. Changing the ammonia concentration in rich solution changes ARS COP and the temperature of absorber; in this context, a concentration value of 33% is recommended. Ambient temperature variations will change the performance of air condensers and increases the pumps working pressure but decreases the COP of ARS. A reduction in CRS cooling rate changes slightly the ARS cooling rate, but HCARS overall COP drops.

Acknowledgements

The partial financial support of Fajr-e-Jam gas refinery in the form of an M.S. thesis joint project for this research is highly appreciated. In addition, the authors would like to express their gratitude for the help and support of the Fajr-e-Jam R&D and engineering departments in carrying out this research.

Nomenclature

0	: Dead (environment or reference) state
A	: Surface
ARS	: Absorption refrigeration system
ARS	: Absortion refrigeration system
COP	: Coefficient of performance
CRS	: Compression refrigeration system
D	: Destruction
e	: Specific energy (kW/kg)
E	: Total exergy of system
HCARS	: Hybrid compression-absorption refrigeration system
HX	: Heat exchanger
L/V	: Liquid/vapor
LP	: Low pressure
$\dot{m}$	: Mass flow rate (kg/s)
NG	: Natural gas
NGL	: Natural gas liquids
P	: Pressure (kPa)

Q	: Heat transfer rate (kW)
s	: Specific entropy (kJ/kg.°C)
T	: Temperature (°C)
V	: Vapor
W	: Power (kW)
X	: Mass fraction
ε	: Specific exergy (kW/kg)

References

Afshar, M. and Rad, H., Exergy Optimization of the Hybrid Compression-absorption Industrial Refrigeration Systems, 8th International Exergy, Energy and Environment Symposium, Antalya, 2016.

Afshar, M. and Rad, H., Simulation and Exergy Analysis of Cascade Absorption Refrigeration System with Heat Recovery of Dew Point Units Waste Heat, 4th Conference of Emerging Trends in Conservation Energy, Tehran, 2015.

Aghniaea, S. and Mahmoudi, S.M., Exergy Analysis of a Novel Absorption Refrigeration Cycle with Expander and Compressor, Indian Journal of Sci. Res., Vol. 1, p. 815-822, 2014.

Andre, M., Sergio, M., Luben, G., and Ricardo, S., Using Engine Exhaust Gas as Energy Source for an Absorption Refrigeration System, International Journal of Applied Energy, Vol. 87, p. 1141–1148, 2010.

Brant, B., Brueske, S., Erickson, D., and Papar, R., Refinery Waste Heat Ammonia Absorption Refrigeration Plant, Journal,Vol. 96, No. 20, p. 61-65, 1998.

Darwish, N., Hashimi, S., and Mansoori, A., A Performance Analysis and Evaluation of a Commercial Absorption-refrigeration Water-ammonia (ARWA) System, International Journal of Refrigeration, Vol. 31, No. 7, p. 1214-1223, 2008.

Erickson, D., Anand, G., and Kyung, I., Heat-activated Dual-function Absorption Cycle, International Journal of ASHRAE Trans, Vol. 110, p. 515-524, 2004.

Fan, Y., Luo, L., and Souyri, B., Review of Solar Sorption Refrigeration Technologies: Development and Applications, Journal of Renew Sustain Energy Rev., Vol. 11, p.1758–1175, 2007.

Garousi, L.F., Mahmoudi, S.M.S., and Rosen, M.A., First and Second Law Analysis of Ammonia/Salt Absorption Refrigeration Systems, International Journal of Refrigeration, Vol. 40, p. 111-121, 2014.

Gas Technology, Technical Information about Natural Gas Cleaning and Treatment, See Also URL http://www.poerner.at/en.html.

Grossman, G. and Zaltash, A., Modular Simulation of Absorption Systems, International Journal of Refrigeration, Vol. 24, No. 6, p. 531-543, 2001.

Janilson, A.R. and Edson, B., Thermodynamic Modeling of an Ammonia-water Absorption System Associated with a Micro-turbine, International Journal of Thermodynamics, Vol. 12, p. 38-43, 2009.

Jianbo, L. and Shiming X., The Performance of Absorption-compression Hybrid Refrigeration Driven by Waste Heat and Power from Coach Engine, International Journal of Applied Thermal Engineering, Vol. 61, p. 747-775, 2013.

Kalinowski, P., Yunho, H., Reinhard, R.., Hashimi, S., and Rodgers, P., Application of Waste Heat Powered Absorption Refrigeration System to the LNG Recovery Process, International Journal of Refrigeration, Vol. 32, p. 687–694, 2009.

Kececiler, A., Acar. H., and Dogan A, Thermodynamic Analysis of Absorption Refrigeration System with Geothermal Energy: an Experimental Study, Journal of Energy Conversion and Management, Vol. 41, p. 37-48, 2009.

Lazzarin, R.M., Gasparella, A., and Longo, G.A., Ammonia-water Absorption Machines for Refrigeration: Theoretical and Real Performances, International Journal of Refrigeration, Vol. 19, No. 4, p. 239-246, 1996.

Liao, X., The Integration of Air-cooled Absorption Chiller in CHP Systems, Ph.D. Thesis, University of Maryland, College Park, MD, USA, 2004.

Lostec, B., Galanis, N., and Millette, J., Simulation of an Ammonia-water Absorption Chiller, International Journal of Renewable Energy, Vol. 60, p. 269-283, 2013.

Manzela, A., Hanriot, S., Cabezas, G., and Sodre, J., Using Engine Exhaust Gas as Energy Source for an Absorption Refrigeration System, International Journal of Applied Energy, Vol. 87, p. 1141–1148, 2010.

Peng, D. and Robinson, D., A New Two-constant Equation of State, Industrial and Engineering Chemistry Fundamentals, International Journal of Chemistry Fundumental, Vol. 15, p. 59-64, 1976.

Priscilla, B., Machado, J., Monterio, J., Medeiros, H., and Epsom, O., Supersonic Separation in Onshore Natural Gas Dew Point Plant, International Journal of Natural Gas and Engineering, Vol. 6, p 43-49,2012.

Pongsid, S., Satha, A., and Supachart, C., A Review of Absorption Refrigeration Technologies, International Journal of Renewable and Sustainable Energy Reviews, Vol. 5, p. 343–372, 2001.

Pratihar, A., Kaushik, S., and Agarwal, R., Performance Evaluation of a Small Capacity Compression-absorption Refrigeration System, International Journal of Applied Thermal Engineering, Vol. 42, p. 41-48, 2012.

Raad, H., Feasibility Study of Hybrid Cooling Systems in Separation of High Molecular Weight Hydrocarbons in Natural Gas, Thesis Submitted to the University of Petroleum University of Technology In Energy Systems Engineering, 2015.

Ruiz, E., Ferro, V.R., Riva, J., Moreno, D., and Palomar, J., Evaluation of Ionic Liquids as Absorbents for Ammonia Absorption Refrigeration Cycles Using COSMO-based Process Simulations, International Journal of Applied Energy, Vol. 123, p. 281–291, 2014.

Srikhirin, P., Aphornratana, S., and Chungpai, S., A Review of Absorption Refrigeration Technologies, Journal of Renewable and Sustainable Energy Reviews, Vol. 5, p. 343–372, 2001.

Takeshita, K., Amano, Y., and Hashizume, T., Experimental Study of Advanced Cogeneration System with

Ammonia-water Mixture Cycles at Bottoming, International Journal of Energy, Vol. 30, p. 247-260, 2005.

Wei, H., Liuli, S., Danxing, Z., Hongguang, J., Sijun, M., and Xuye, J., New Hybrid Absorption-compression Refrigeration System Based on Cascade Use of Mid-temperature Waste Heat, International Journal of Applied Energy, Vol. 106, p. 383–390, 2013.

Zare, V., Mahmoudi, S.M., Yari, M., and Amidpour, M., Thermoeconomic Analysis and Optimization of an Ammonia-water Power/Cooling Cogeneration Cycle, International Journal of Energy, Vol. 47, p. 271-283, 2012.